Chemical Transport Synthesis, Electrochemical Behavior, and Electronic Structure of Superconducting Zirconium and Hafnium Nitride Halides

Mikhail Vlassov,[†,‡] M. Rosa Palacín,[†] Daniel Beltrán-Porter,[§] Judith Oró-Solé,[†] Enric Canadell,[†] Pere Alemany,[⊥] and Amparo Fuertes*[,†]

Institut de Ciència de Materials de Barcelona (CSIC), Campus UAB, 08193 Bellaterra, Spain, Institut de Ciència de Materials de la Universitat de València, P.O. Box 2085, 46071 València, Spain, and Departament de Química-Física, Facultat de Química, Universitat de Barcelona, Diagonal 647, 08028 Barcelona, Spain

Received March 18, 1999

The layered nitrides β-MNX (M = Zr, Hf; X = Cl, Br) crystallize in the space group $R\bar{3}m$ with a hexagonal cell of dimensions $a = 3.6031(6)$ Å, $c = 27.672(2)$ Å for β-ZrNCl, $a = 3.5744(3)$ Å, $c = 27.7075(9)$ Å for β-HfNCl, and $a = 3.6379(5)$ Å, $c = 29.263(2)$ Å for β-ZrNBr. Lithium intercalation using *n*-buthyllithium in hexane solutions leads to solvent free superconductors of formula $Li_{0.20}ZrNCl$, $Li_{0.42}HfNCl$, $Li_{0.67}HfNCl$, and $Li_{0.17}ZrNBr$ showing critical temperatures of 12, 18, 24, and 13.5 K, respectively. Whereas several samples of β-ZrNBr and β-ZrNCl showed reproducibility in the lithium uptake and in the corresponding critical temperatures, different samples of β-HfNCl subjected to the same treatment in *n*-buthyllithium showed lithium uptakes ranging from 0.07 to 0.67, and corresponding critical temperatures between 0 and 24 K. A linear dependence of T_c versus the lithium content is observed when all the superconducting samples are considered. The results obtained from electrochemical lithiation are consistent with those obtained with chemical methods, as samples with larger capacity on discharge are also those found to have larger lithium contents after chemical lithiation. Most samples present a reduction step around 1.8 V vs Li^0-Li^+ whose origin is still unclear. The electrochemical capacity on discharge for β-HfNCl and β-ZrNBr depends on the milling time spent in the preparation of the electrodes, with long milling times resulting in lower intercalation degree. Possible causes for this effect are either the creation of structural defects (e.g., stacking faults) or some sample decomposition induced by local heating. The same phenomena are proposed to account for the different behavior of β-HfNCl samples, although additional aspects such as the presence of hydrogen, oxygen, or extra hafnium atoms in the structure have to be considered. Tight-binding band structure calculations for β-MNX (M = Zr, X = Cl, Br; M = Hf, X = Cl), ZrCl, and $Y_2C_2Br_2$ are reported. The density of states and Fermi surfaces of the β-MNX phases as well as the relationship between the electronic structure of the β-ZrNCl and ZrCl are discussed. Despite the structural relationships, the electronic structures near the Fermi level of the β-MNX and $Y_2Br_2C_2$ phases are found to be very different.

Introduction

The recently discovered layered intercalated compounds M_xZrNCl, M_xZrNBr, and M_xHfNCl (M = alkaline ion) represent a new class of ionocovalent superconductors with record critical temperatures for inorganic non-oxide materials.[1−3] The structure of the host lattices of those phases was first reported by Juza et al. in 1964,[4] and recently redetermined in a supercell with the new space group $R\bar{3}m$.[3,5,6] The layered compounds β-MNX (M = Hf, Zr; X = Cl, Br) crystallize in the rhombohedral *SmSI* structure.[7] They are built up by double layers of composition −X(MNNM)X− stacking along *c* that are separated by a van der Waals gap where different species can be intercalated.[1−3,8] All atoms are located in 6c sites (0,0,*z*) with approximate *z* of 0.12, 0.20, and 0.39 for M, N, and X, respectively. The cell parameters are $a \cong 3.6$ Å and $c \cong 27.7$ Å (for X = Cl) and 29.3 Å (for X = Br). The Zr or Hf metal atoms are bonded to three halide atoms from outside the layer (d(M−X) ≅ 2.7 Å for X = Cl and 2.9 Å for X = Br), three nitrogen atoms inside the layer (d(M−N) ≅ 2.1 Å), and one additional nitrogen from the second N sheet (d(M−N) ≅ 2.2−2.3 Å) (Figure 1a).[3] The coordination polyhedra described by these ligands is a single capped trigonal antiprism. The new structure may be considered as a result of the intercalation of N atoms in the tetrahedral sites of the ZrCl structure. ZrCl shows the same space group $R\bar{3}m$ and similar cell parameters ($a = 3.424(2)$ Å and $c = 26.57(4)$ Å) (see Figure 1b).[9,10] The structure of the layered mono-

[†] Institut de Ciència de Materials de Barcelona (CSIC).
[‡] Permanent address: Earthcrust Research Institute, St. Petersburg University, Russia.
[§] Institut de Ciència de Materials de la Universitat de València.
[⊥] Universitat de Barcelona.

(1) Yamanaka, S.; Hohetama, K.; Kawaji; H. *Nature* **1998**, *392*, 580−582.
(2) (a) Yamanaka, S.; Kawaji, H.; Hotehama, K.; Ohashi, M. *Adv. Mater.* **1996**, *8*, 771. (b) Kawaji, H.; Hotehama, K.; Yamanaka, S. *Chem. Mat.* **1997**, *9*, 2127.
(3) Fuertes, A.; Vlassov, M.; Beltrán-Porter, D.; Alemany, P.; Canadell; Casañ-Pastor, N.; Palacín, M. R. *Chem. Mater.* **1999**, *11*, 203.
(4) Juza, R.; Friedrichsen, H. *Z. Anorg. Allg. Chem.* **1964**, *332*, 173−178.
(5) Fogg, A. M.; Evans, S. O.; O'Hare, D. *Chem. Commun.* **1998**, 2269.
(6) Shamoto, S.; Kato, T.; Ono, Y.; Miyazaki, Y.; Ohoyama, K.; Ohashi, M.; Yamaguchi, Y.; Kajitani, T. *Physica C* **1998**, *306*, 7.
(7) Hulliger, F. In *Structural Chemistry of Layer-Type Phases*; Lévy, F.; Ed.; D. Reidel Publishing Co.: Dordrecht/Boston, 1976; Vol. 5, p 263.
(8) Fogg, A. M.; Green, V. M.; O'Hare, D. *Chem. Mater.* **1999**, *11*, 216.
(9) Adolphson, D. G.; Corbett, J. D. *Inorg. Chem.* **1976**, *15*, 1820.

10.1021/ic9903127 CCC: $18.00
Published on Web 09/15/1999

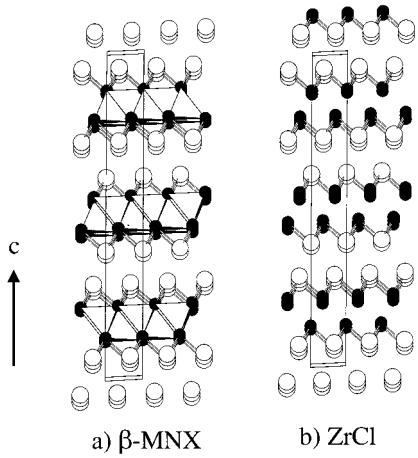

Figure 1. Crystal structures of (a) the host lattice for the superconductors Li_xMNX (M = Zr, Hf; X = Cl, Br)[3] and (b) ZrCl.[9] Black and white spheres represent metal and halide atoms, respectively. Nitrogen atoms are placed at the center of the tetrahedra.

halides MX (M = Sc, Zr, Hf, Y, Ln; X = Cl, Br) consists of cubic-close-packed layers of metal and halide atoms stacked in pairs, yielding the sequence X−M−M−X with relative orientations *AbcA*. They span metallic behavior from the physical and chemical points of view. The basic structure of the monohalide is preserved after oxidative chemical reactions, leading to $M_2X_2Z_2$ or M_2X_2Z (M = Sc, Y, Ln; Z = H, C) and MXZ or $MXZ_{0.5}$ (M = Zr, Hf; Z = H, C, O, N), where the nonmetal atoms (Z) occupy interstitial sites in the double metal layers.[11−13] In the zirconium halide derivatives, the anions O^{2-} (in $ZrClO_{0.5}$),[13] C^{4-} (in $ZrClC_{0.5}$),[14] H^- (in Zr_2X_2H),[15] and N^{3-} (in β-ZrNX)[3] occupy the tetrahedral sites, whereas in the lanthanide derivatives the Z anions occupy either the tetrahedral or the octahedral sites. The insertion of anions modifies the band population and affects the electronic properties, the result being normal valence or semiconducting compounds. As in the alkaline-intercalated β-MNX compounds, superconductivity has also been recently reported for the ternary lanthanide carbide halides $Ln_2C_2X_2$ (Ln = La, Y, Lu; X = Br, I) as well as for their thorium-substituted or sodium-intercalated derivatives.[16]

The intercalation of alkaline ions in β-ZrNCl either chemically or electrochemically has been investigated since 1984 by Yamanaka et al. because of the potential application of this compound as insertion electrode or electrochromic material.[17−19] More recently, the same authors reported superconductivity below 12 K for the lithium-inserted compound $Li_{0.2}ZrNCl$, and below 25 K for the intercalated hafnium derivative Li_xHfNCl.[2,1] Co-intercalation of organic molecules takes place in polar solvents such as tetrahydrofuran (THF), dimethylformamide (DMF), or propylene carbonate (PC). This can be done either during the intercalation reaction of alkaline ions or by additional treatment in the organic solvent of the intercalated phases.[1,2] The co-intercalation process allows an increase of the alkali metal uptake because of the concomitant larger separation between the layers in the van der Waals gap, but the doping mechanism and the physical properties of the resulting superconductors may be different from those of the solvent free materials. Cobaltocene intercalation on β-ZrNCl leads to superconducting materials with the same doping levels and critical temperatures as those observed in the alkali metal intercalates.[8]

In a recent communication[3] we reported the crystal structures for the host compounds β-HfNCl, β-ZrNCl, and β-ZrNBr, as well as superconductivity below 13.5 K for $Li_{0.17}ZrNBr$ and preliminary band structure calculations. In the same paper superconductivity below 24 K in solvent free Li_xHfNCl was also reported for the first time. In this paper we present a comparative study of the synthesis, chemical lithiation and electrochemical behavior for different samples of the solvent free superconductors Li_xZrNCl, Li_xHfNCl, and Li_xZrNBr. We also report electronic band structure calculations for the three corresponding host compounds, and comment on the relationship between their electronic structures and that of the parent compound ZrCl.

Experimental Section

Synthesis of Zirconium and Hafnium Nitride Halides. β-HfNCl, β-ZrNCl, and β-ZrNBr were prepared by the reaction of Hf (Aldrich, 99.5%) or Zr (Alfa, 99.9%) with NH_4Cl (Aldrich, 99.9%) or NH_4Br (Aldrich, 99.999%) at 850 °C, followed by recrystallization via vapor transport under conditions reported previously.[3,20] Whereas for β-ZrNCl and β-ZrNBr we obtained reproducibility in the electrochemical or chemical intercalation behavior, samples with different intercalation capacities were obtained for β-HfNCl using similar conditions in the synthesis (hereafter labeled HfNCl-I to HfNCl-V). The sample HfNCl-II was recrystallized just by treatment at 850 °C without chemical vapor transport.

Chemical Intercalation. Chemical lithiation reactions were done between room temperature and 50° C by dispersion of the powders in a 0.1 M solution of *n*-buthylithium in hexane (Aldrich), using evacuated Ar-sealed glass tubes. The lithiation time was 140 h. Lithium contents were determined by atomic emission analysis. Before lithiating the samples, elemental analysis was performed to determine N and H contents.

Electrochemical Intercalation. Electrochemical tests were made with Swagelok cells. The positive electrode was prepared by manually grinding the sample with 30 wt % black carbon (SP kindly supplied by MMM, Belgium). To investigate the effect of grinding on the capacity for discharge, different milling times were used in some cases for two independent portions of the same sample. Two sheets of Whattman GF/D borosilicate glass fiber, soaked with 1 M $LiPF_6$ in 1:1 EC/DMC (ethylene carbonate/dimethyl carbonate) electrolyte, were used as a separator. The negative electrode consisted of lithium metal foil (0.38 mm thick). Cells were tested on an Arbin BT2042 cycler operating in a galvanostatic low-current mode between 3 and 1.25 V and at a rate of 1 Li atom/200 h. Handling of the lithiated samples and cell preparation were done in an Ar-filled glovebox.

X-ray Diffraction, Electron Diffraction, and Transmission Electron Microscopy. X-ray diffraction patterns were taken in Seifert 3000 and Siemens D-5000 diffractometers using Cu Kα radiation. Profile refinements, using the Rietveld method, were carried out with the help of the program FULLPROF.[21] Electron diffraction patterns, electron

(10) Ford, J. E.; Corbett, J. D.; Hwu, S. *Inorg. Chem.* **1983**, *22*, 2789 and references therein.
(11) Corbett, J. D.; McCarley, R. E. New Transition Metal Halides and Oxides. *Crystal Chemistry and Properties of Materials with Quasi-One-Dimensional Structures*; Rouxel, J., Ed.; Reidel Publishing: Dordrecht/Boston, 1986.
(12) Meyer, G.; Hwu, S.; Wijeyesekera, S.; Corbett, J. D. *Inorg. Chem.*, **1986**, 25, 4811.
(13) Seaverson, L. M.; Corbett, J. D. *Inorg. Chem.* **1983**, *22*, 3202.
(14) Ford, J.; Corbett, J. D.; Hwu, S. *Inorg. Chem.* **1983**, *22*, 2790.
(15) Wijeyesekera, S. D.; Corbett, J. D. *Inorg. Chem.* **1986**, *25*, 4709.
(16) Henn, R. W.; Schnelle, W.; Kremer, R. K. and Simon, A. *Phys. Rev. Lett.* **1996**, *77*, 374, and references therein.
(17) Yamanaka, S.; Kawaji, S.; Sumihara, M.; Hattori, M. *Chem. Lett.* **1984**, 1403.
(18) Ohashi, M.; Yamanaka, S.; Sumihara, M.; Hattori, M. *J. Incl. Phenom.* **1984**, *2*, 289.
(19) Ohashi, M.; Shigeta, T.; Yamanaka, S.; Hattori, M. *J. Electrochem. Soc.* **1989**, *136*, 1086.
(20) Ohashi, M.; Yamanaka, S.; Sumihara, M.; Hattori, M. *J. Solid State Chem.* **1988**, *75*, 99.
(21) Rodríguez-Carvajal, J. Program FULLPROF, Version 2.5, April 1994, Institut Laue-Langevin, unpublished.

Table 1. Exponents and Parameters Used in the Calculations

atom	orbital	H_{ii} (eV)	ζ_1	ζ_2	c_1[a]	c_2[a]
Zr	5s	−6.41	1.82			
	5p	−3.77	1.78			
	4d	−6.97	3.84	1.51	0.6210	0.5769
Hf	6s	−6.61	2.21			
	6p	−3.84	2.17			
	5d	−6.90	4.36	1.71	0.6967	0.5322
Y	5s	−6.01	1.74			
	5p	−3.62	1.70			
	4d	−5.74	1.56	3.55	0.8213	0.3003
Cl	3s	−26.64	2.18			
	3p	−14.22	1.73			
Br	4s	−25.21	2.59			
	4p	−12.96	2.13			
N	2s	−25.37	1.95			
	2p	−13.90	1.95			
C	2s	−19.65	1.63			
	2p	−11.13	1.63			

[a] Contraction coefficients used in the double-ζ expansion.

microscopy images, and XEDS analyses were obtained in a JEOL 1210 transmission electron microscope operating at 120 kV, equipped with a side-entry 60/30° double tilt GATHAN 646 analytical specimen holder and a Link QX2000 XEDS element analysis system. The specimens for electron microscopy were prepared by dispersion of the powders in *n*-heptane and deposition of a droplet of this suspension on a carbon-coated holey film supported on an aluminum grid. The particle sizes were estimated by observation of low-resolution transmission electron images for a minimum of 50 crystals of each sample.

Magnetic Susceptibility. Magnetic susceptibility measurements were performed in a Quantum Design SQUID magnetometer down to 5 K, on the lithiated powder samples double sealed under Ar atmosphere, in zero-field-cooled and field-cooled conditions (H_{measd} = 30 G).

Band Structure Calculations. The tight-binding band structure calculations use an extended Hückel Hamiltonian[22] and a modified Wolfsberg−Helmoltz formula[23] to calculate the nondiagonal H_{ij} matrix elements. Except otherwise stated, a rigid band scheme was used to analyze the effect of the lithiation. The exponents and parameters[24] used in the calculations are summarized in Table 1.

Results and Discussion

Synthesis, Crystal Chemistry, and Superconducting Properties. All the samples that were purified by vapor transport in the last step of the synthesis (HfNCl-I, HfNCl-III, HfNCl-IV, HfNCl-V, β-ZrNCl, and β-ZrNBr) showed impurity free X-ray diffraction patterns that can be indexed in a hexagonal cell of dimensions a = 3.6031(6) Å, c = 27.672(2) Å for β-ZrNCl, a = 3.5744(3), c = 27.7075(2) Å for β-HfNCl, and a = 3.6379(5), c = 29.263(2) Å for β-ZrNBr, with the space group $R\bar{3}m$.[3] Figure 2 shows the observed and calculated X-ray diffraction patterns for β-ZrNCl performed with the program FULLPROF.[3] Similar figures corresponding to the pure compounds β-HfNCl and β-ZrNBr are reported in ref 3. The X-ray diffraction pattern of the sample HfNCl-II showed small impurities of HfO_2 and Hf_2ON_2 (see Figure 3), but its crystallinity degree and purity were found to be significantly higher than those of the nontransported samples, i.e., those obtained after the reaction of Hf or Zr with ammonium halide, without further recrystallization. Table 2 shows the lithium intercalation degrees, hydrogen contents, particle sizes, and critical temperatures for the different samples.

For β-ZrNCl and β-ZrNBr compounds, reproducibility in the synthesis and in the intercalation behavior was observed. Indeed,

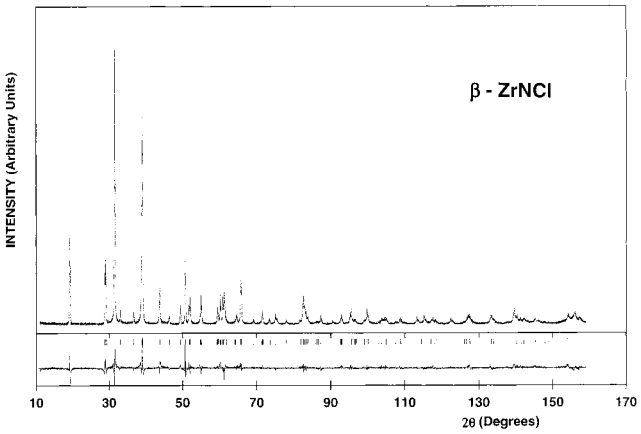

Figure 2. Observed and calculated X-ray diffraction patterns for β-ZrNCl.[3]

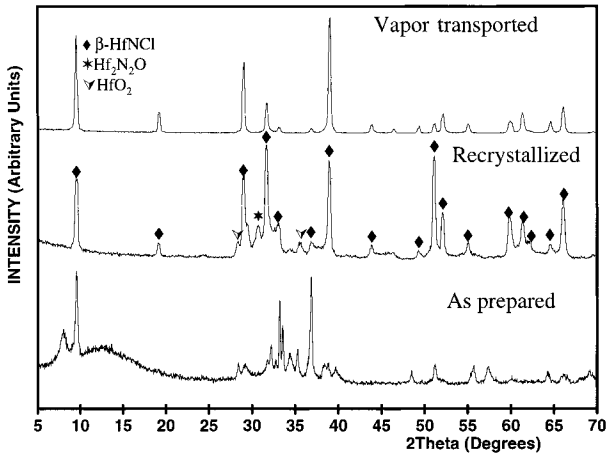

Figure 3. Powder X-ray diffraction patterns of β-HfNCl samples as prepared after the reaction of Hf and NH_4Cl, recrystallized at 850 °C (HfNCl-II), and chemical vapor transported.

different samples obtained in the same synthesis conditions led to the same lithium uptakes upon treatment with *n*-buthyllithium, similar electrochemical behaviors, and the same critical temperatures. In contrast, β-HfNCl samples showed significant differences in behavior. The amount of lithium intercalated after 140 h of treatment with *n*-buthyllithium was ≤0.11 per formula unit for HfNCl-IV and HfNCl-V whereas HfNCl-I and HfNCl-III showed a significantly higher lithium uptake, 0.67 and 0.42, respectively. The color of the samples changed to dark gray or black upon lithium intercalation. Lithiated HfNCl-IV and HfNCl-V did not show any superconducting transition down to 4 K, whereas lithiated HfNCl-I, HfNCl-II, and HfNCl-III showed critical temperatures of 24, 18, and 18 K, respectively. The observation of a T_c of 18 K for a lithium content lower than 0.67 differs remarkably from that found for samples treated with naphthyllithium in the previous work from Yamanaka et al.[1] In that case, the solvent tetrahydrofuran (THF) was systematically co-intercalated with lithium in the van der Waals gap, and consequently their samples were formulated as $Li_x(THF)_yHfNCl$. In these samples the critical temperatures varied only from 25.5 to 24.4 K for a wide range of lithium contents, i.e., between y = 0.13 and y = 0.97. This difference in behavior suggests that the co-intercalated molecules may play a role in the charge-transfer process, and that a different doping mechanism may operate in the superconducting solvent free compounds. Compared to Li_xHfNCl, the solvent free zirconium samples allowed a lower intercalation level. For the two compounds Li_xZrNCl and Li_xZrNBr only one superconducting

(22) Whangbo, M.-H.; Hoffmann, R. *J. Am. Chem. Soc.* **1978**, *100*, 6093.
(23) Ammeter; J.; Bürgi; H.-B; Thibeault, J.; Hoffmann, R. *J. Am. Chem. Soc*. **1978**, *100*, 3686.
(24) Vela; A.; Gázquez, J. L. *J. Phys. Chem*. **1988**, *92*, 5688.

Table 2. Particle Sizes, Chemical Analysis, and Critical Temperatures for MNX

sample MNX	color	particle size (for ~70% of crystals) (μm)	no. of H atoms/formula	x (Li uptake)	T_c (onset) (K)
HfNCl-I	light gray	<1.5		0.67	24
HfNCl-II	light gray	<1	0.38	0.17[a]	18
HfNCl-III	light gray	<1.5		0.42	18
HfNCl-IV	dark gray, metal brightness	<1.5	0.32	0.07	0
HfNCl-V	dark gray, metal brightness	>5	0.0	0.11	0
β-ZrNCl	yelow greenish	<2	0.32	0.20	12
β-ZrNBr	golden	<2	0.22	0.17	13.5

[a] Due to the presence of impurities, this value has to be taken as lower than the true one.

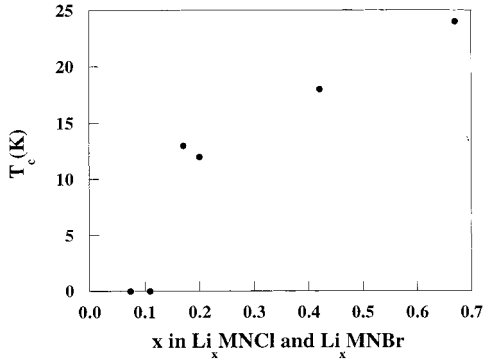

Figure 4. T_c (onset) versus lithium contents in Li_xMNCl and Li_xMNBr samples prepared by treatment with *n*-buthyllithium.

phase with $x \cong 0.2$ and a critical temperature of 12−13 K was found. In Figure 4 we have plotted the transition temperature for all the intercalated phases of pure samples of β-ZrNCl, β-ZrNBr, and β-HfNCl, versus the lithium content (x). A linear dependence of T_c with x is observed for lithium contents between 0.17 and 0.67, and the samples with x lower than 0.17 did not show superconductivity. It seems then that, in the absence of intercalated solvent, a correlation exists between the observed T_c and the amount of lithium in the van der Waals gap (i.e., the transferred electrons) that does not depend either on the transition metal (Zr or Hf) or on the halide (Cl and Br). The three compounds β-ZrNCl, β-ZrNBr, and β-HfNCl contain hydrogen, in an amount lower than 0.38 atom per formula. For Hf samples, the amount of lithium intercalated does not seem to be related with the hydrogen content, since samples with 0.32 hydrogen atom per formula unit or without hydrogen show similar lithium contents and magnetic susceptibility behavior. This is consistent with the results described in a previous work by Kawaji et al. for β-ZrNCl, suggesting that these H atoms are bonded to N atoms in the double layers M−N−N−M and are not placed in the van der Waals gap.[25]

In Figure 5 we show electron microscopy images obtained for different samples of β-HfNCl, and in Figure 6 the electron diffraction patterns along the zone axis [100] for β-ZrNCl, β-ZrNBr, and β-HfNCl are reported. The particles show hexagonal platelet morphologies, and strong preferential orientation with the c axis nearly parallel to the electron beam. In general a broad distribution of particle sizes was observed, these being lower than 2 μm for HfNCl-I to HfNCl-IV, β-ZrNCl, and β-ZrNBr, and up to 11 μm for HfNCl-V. The hafnium samples showed differences in color, and some of them exhibited metal brightness. The electron diffraction patterns along [100] for the three compounds showed streaking and diffuse lines parallel to [001]*, indicating disorder in the stacking of the layers along the c direction. This disorder was more important in β-ZrNBr than in β-ZrNCl or β-HfNCl, and was also evident in the X-ray diffraction patterns by the presence of strong asymmetric broadening in reflections corresponding to 10*l*, 01*l*, and 20*l*, and normal shape for 00*l* and 11*l* peaks.

Electrochemical Behavior. As stated above, the electrochemical properties of β-ZrNCl were first studied by Yamanaka et al.[19] These authors found out that β-ZrNCl is able to intercalate about 0.2 lithium atom per formula unit, and they reported two different types of electrochemical behavior: in the samples recrystallized by vapor transport, a reduction step at about 1.8 V was observed whereas no definite reduction step could be seen before the transport reaction (only a gradual voltage decrease in the volts vs x galvanostatic curve).

We have carried out electrochemical tests in a galvanostatic mode for the whole series of β-HfNCl samples prepared under different conditions and also for β-ZrNCl and β-ZrNBr. These tests, similar to those previously reported,[19] have been carried out under the conditions normally used for lithium batteries, and thus using a liquid organic electrolyte. This technology has proved to have some inconveniences when applied to the materials under study. First of all, as these compounds are able to intercalate polar organic molecules, there is certainly a co-intercalation of the electrolyte solvent with lithium. This fact may have an effect on the reversibility of the electrochemical process, and moreover it prevents detailed comparison with the chemical lithiation that takes place in hexane and thus without co-intercalation. On the other hand, these materials show low lithium intercalation potentials, but the study at very low potentials is hindered because reduction of the liquid electrolyte begins below 1.5 V vs Li. A blank experiment was performed with an electrode containing only SP carbon to estimate a potential limit under which the extent of electrolyte reduction is too important (see Figure 7). Taking these results into account, we performed the electrochemical experiments down to 1.25 V; after this value the electrolyte reduction prevents the obtention of any significant data from the sample. Efforts to solve this problem are in progress with the use of a different technology with a polymer electrolyte that should allow the electrochemical study up to 0 V vs Li and obviously without co-intercalation.

The curve corresponding to the electrochemical reduction of β-ZrNCl is shown in Figure 7. The sample was found to intercalate 0.24 lithium atom down to 1.25 V, and an electrochemical reduction step is observed at about 1.8 V, results that are consistent with previous observations.[19]

Concerning the β-HfNCl series, the most striking result is the great difference both in the shape of the curves and in the degree of lithium intercalation of the samples (see Figure 8). Indeed, samples I and III intercalate 0.43 and 0.34 lithium atom per formula unit down to 1.25 V whereas the values are 0.14 and 0.12 for samples IV and V, respectively. Sample II constitutes a special case, as x values cannot be determined due to the fact that it contains impurities, and the curve has only been included in the graph for the sake of shape comparison.

(25) Kawaji, H.; Yamamoto, K.; Yamanaka, S.; Ohashi, M. *J. Coord. Chem.* **1996**, *37*, 77.

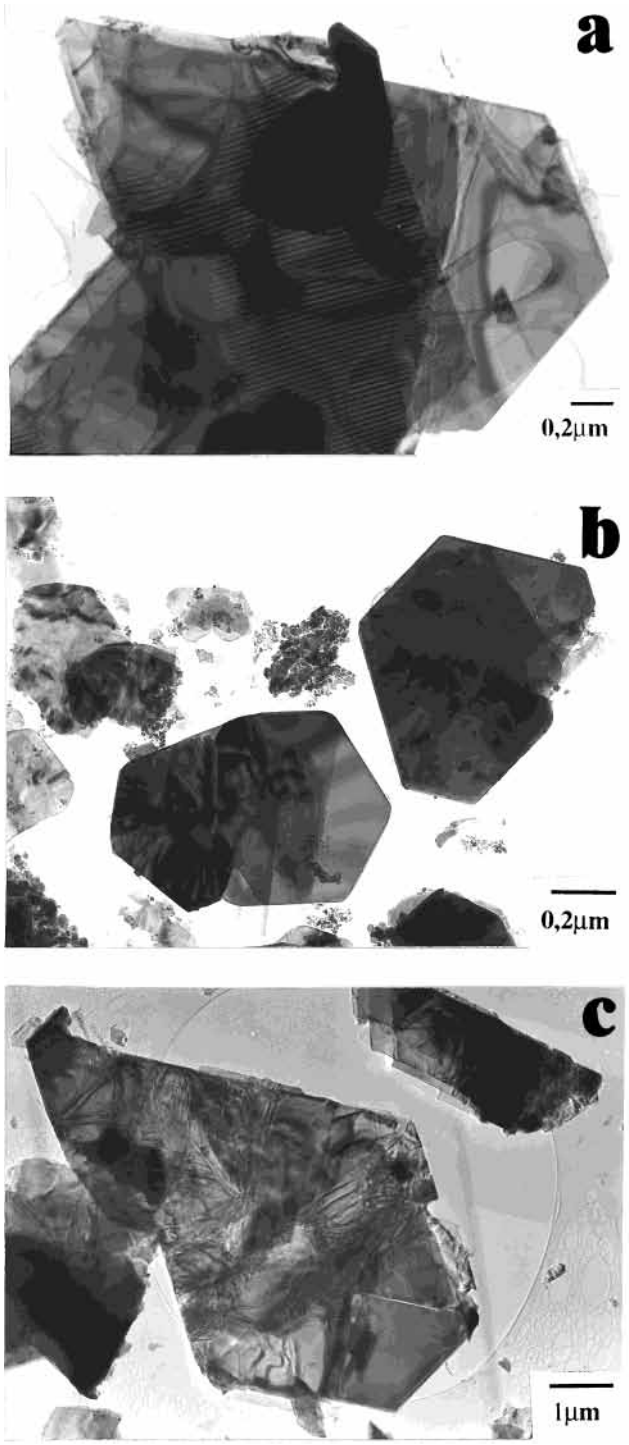

Figure 5. Transmission electron microscopy micrographs for the samples (a) HfNCl-I, (b) HfNCl-II, and (c) HfNCl-V.

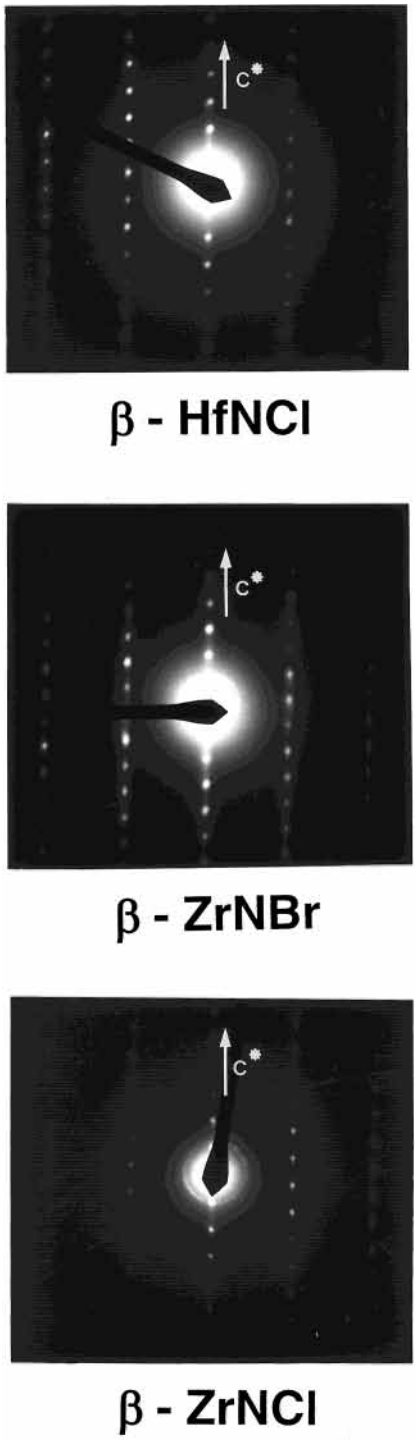

Figure 6. Electron diffraction patterns along the [100] axes for β-ZrNCl, β-ZrNBr, and β-HfNCl.

In summary, electrochemical data are consistent with the data obtained from chemical lithiation, as superconducting samples are those showing high lithium intercalation ability. Moreover, sample I, which is the one exhibiting the highest T_c (24 K), presents the largest electrochemical capacity on discharge.

The curve corresponding to β-ZrNBr is shown in Figure 7. In this case, the reduction of the electrolyte seems to begin at potentials slightly higher than in all the other samples studied, and thus the degree of lithium intercalation below 1.5 V cannot be measured. However, it intercalates 0.12 lithium atom up to 1.5 V, thus presenting a behavior somewhat similar to that of HfNCl-III.

In general, there is a good correlation between the results of the electrochemical and the chemical intercalation for all samples. However, and as previously reported[19] for β-ZrNCl, two types of distinct electrochemical curves are also found in our study. Indeed, the reduction step at about 1.8 V is observed for some samples, namely, β-ZrNCl, HfNCl-I, and HfNCl-III. On the contrary, it does not appear for HfNCl-II, HfNCl-IV, HfNCl-V, and β-ZrNBr. The reason for this difference in behavior is not clear. Ohashi et al.[19] correlated it to the crystallinity of the sample as only transported (i.e., more pure and crystallized) samples showed the step at 1.8 V. In the case of the samples analyzed in this study, such a correlation is not

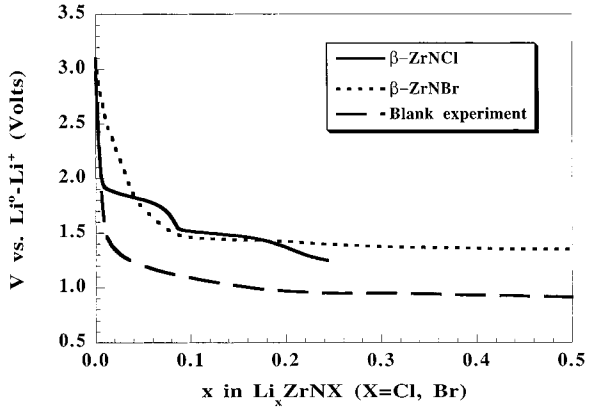

Figure 7. Galvanostatic curves corresponding to lithium intercalation in β-ZrNCl and β-ZrNBr. The result of a blank experiment made with an electrode without active material is also shown.

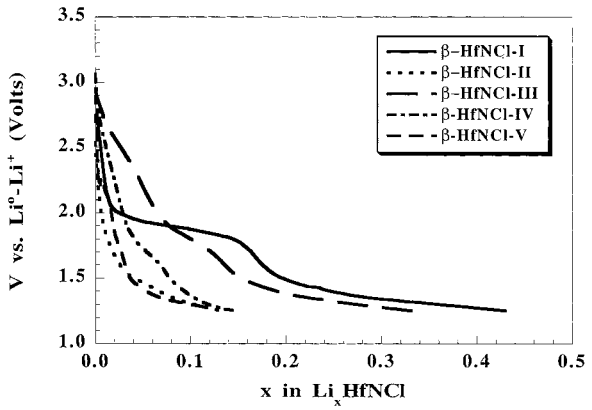

Figure 8. Galvanostatic curves corresponding to lithium intercalation in the samples resulting from the diverse synthesis of β-HfNCl.

so easy to draw. Further studies are in progress to ascertain the origin of this reduction step.

Effect of Grinding on the Electrochemical Behavior. The degree of lithium intercalation was found to depend also on the milling time spent in the preparation of the mixtures with SP carbon for β-HfNCl and β-ZrNBr but not for β-ZrNCl. A long milling time results in a more homogeneous mixture, but it seems to hinder lithium intercalation in β-HfNCl and β-ZrNBr. See for instance Figure 9. This effect might be due to the creation of structural defects in the milling process. The presence of stacking faults, for instance, could avoid the lithium diffusion into the van der Waals gap and, consequently, play a crucial role in the electrochemical activity. A related behavior has been observed and described in detail by Chabre and Pannetier for the intercalation of protons in manganese dioxide.[26] Similarly, the presence of structural defects affects considerably the electrochemical activity of layered $Ni(OH)_2$.[27,28] A second possible cause for the lowering of the electrochemical capacity of discharge after long milling is some sample decomposition induced by local heating. Although no impurities are seen in the X-ray diffraction patterns of ground samples, secondary phases could be present in low proportion in the surface of the crystallites, thus preventing the lithium diffusion into the van der Waals gap. The same phenomena could explain the differences in the chemical and electrochemical intercalation behavior observed in β-HfNCl samples (i.e, HfNCl-I to HfNCl-V) (vide ante). However, in that case additional aspects such as the chemical composition (presence of hydrogen, oxygen, or extra Hf intercalated in the van der Waals gap) have to be taken into account. The relative influence of all these possible factors is currently under study.

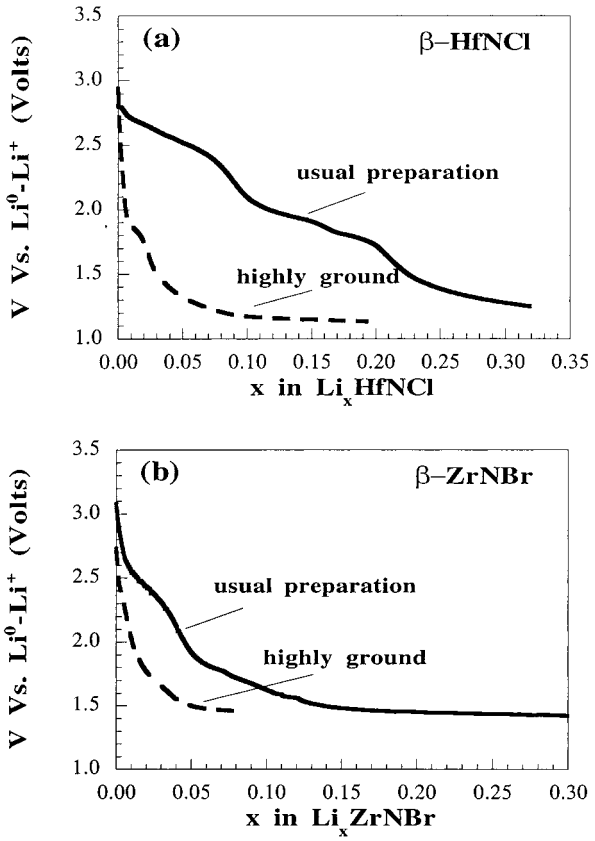

Figure 9. Galvanostatic curves corresponding to lithium intercalation in (a) β-HfNCl and (b) β-ZrNBr, both with the usual electrode preparation method and for highly ground portions of the same samples.

Electronic Structure. In this section we comment on the relationship between the crystal and electronic structures of these new superconducting nitrides. More specifically, we consider the relationship between the electronic structure of the host lattice β-ZrNCl and the "parent" ZrCl lattice as well as the adequacy of a rigid band scheme in studying the electronic structure of the intercalated phases.

As stated above, the β-ZrNCl[3,5,6] and ZrCl[9] phases crystallize in the same group ($R\bar{3}m$), with very similar cell parameters. The Zr and Cl atoms lie in 6c sites (0,0,z) with very similar z values. Thus, the β-ZrNCl phase can be viewed as a nitride intercalation compound of ZrCl where the N atoms occupy the tetrahedral intralayer sites (see Figure 1). The calculated densities of states (DOS) for the layers found in the ZrCl and β-ZrNCl phases are reported in parts a and b, respectively, of Figure 10. In Figure 10a (ZrCl), 16 electrons fill the states below the energy gap around -10 eV (the unit cell of a layer contains 2 formula units) and 6 electrons are left to fill the states above the energy gap, which are mainly Zr in nature. In Figure 10b (β-ZrNCl), the Fermi level lies on the energy gap around -10 eV and 32 electrons fill the levels below it. Upon intercalation, the levels above the gap, which are also mainly Zr in nature, become filled although much less than in ZrCl (i.e., 2x electrons for Li$_x$ZrNCl but 6 in ZrCl). Thus, from a purely formal viewpoint, one could naively think that intercalation in the β-ZrNCl phases is just a convenient way to reach lower electron counts favorable for the appearance of superconductivity in the

(26) Chabre, Y.; Pannetier, J. *Prog. Solid. State Chem.* **1995**, *23*, 1.
(27) Bernard, M. C.; Bernard, P.; Keddam, M.; Senyarich, S.; Takenouti, H. *Electrochim. Acta* **1996**, *41*, 91.
(28) Delmas, C.; Tessier, C. *J. Mater. Chem.* **1997**, *7*, 1439.

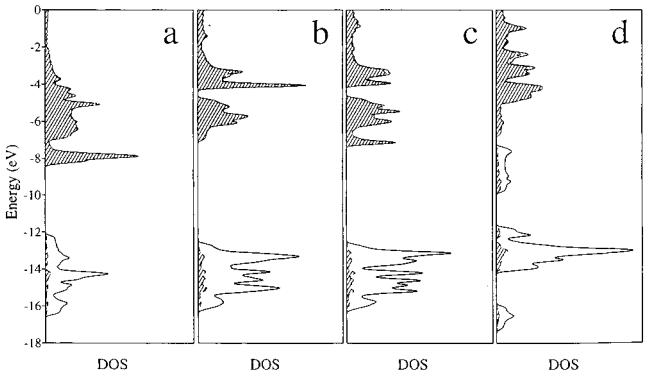

Figure 10. Calculated density of states (DOS) and transition-metal-projected DOS (shaded region) for a layer of (a) ZrCl, (b) β-ZrNCl using the redetermined structure, (c) β-ZrNCl using the structure of Juza et al.,[4] and (d) $Y_2C_2Br_2$.

ZrCl lattice. However, this would be incorrect because simple inspection of the DOS curves in Figure 10a,b suggests that the levels above the energy gap (i.e., those which will be partially filled and responsible for the conductivity in ZrCl and Li_xZrNCl) must be quite different in character.

The coordination environment of Zr in ZrCl[9] contains three Cl atoms at 2.63 Å and three Zr atoms at 3.09 Å as well as six extra Zr atoms at 3.42 Å (see **1**, where the six extra Zr atoms

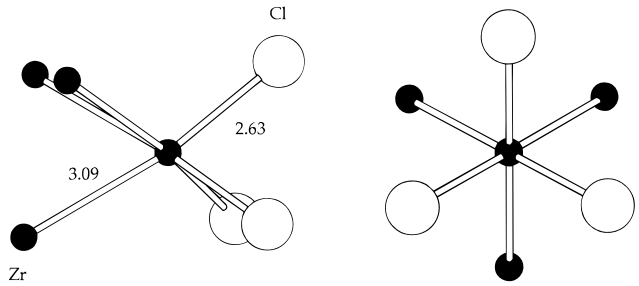

1a **1b**

have not been shown for clarity). In β-ZrNCl[3] the coordination environment of the Zr atom contains three Cl atoms at 2.76 Å, three N atoms at 2.12 Å, one N atom at 2.24 Å, and three Zr atoms at 3.35 Å (see **2a** and **2b** for two views with and without

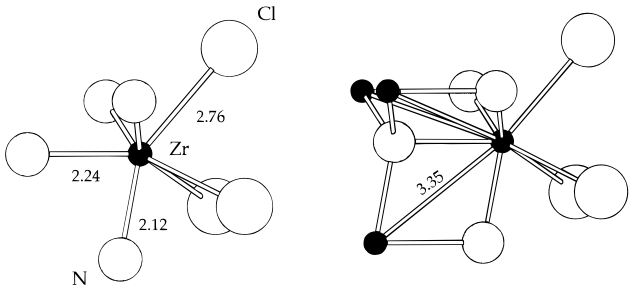

2a **2b**

the coordinated Zr atoms). Six extra Zr atoms lie at 3.60 Å. Such different coordination environments must lead to a considerably different electronic structure. For instance, the calculated overlap populations for Zr−Cl, Zr−Zr (3.09 Å) and Zr−Zr (3.42 Å) in ZrCl are 0.312, 0.462, and 0.126, respectively. Thus, it is clear that there is extensive metal−metal bonding in ZrCl. Most of this metal−metal bonding comes from the filling of the states above the energy gap so that the metallic behavior of ZrCl is the result of this extended metal−metal bonding. The calculated overlap populations for Zr−Cl, Zr−Zr (3.35 Å), Zr−Zr (3.60 Å), Zr−N (2.12 Å), and Zr−N (2.24 Å) in β-ZrNCl are 0.261, −0.006, −0.008, 0.324, and 0.267, respectively. The absence of metal−metal interactions is not just the result of emptying the states above the energy gap in β-ZrNCl. Calculations for the ZrCl sublattice of β-ZrNCl as a function of the number of electrons filling the states above the energy gap give Zr−Zr overlap populations not very different from those obtained for ZrCl itself (especially for the shorter Zr−Zr distance). Thus, introduction of the N atoms into the ZrCl double layer to give the β-ZrNCl lattice leads to severe modifications in the d-block bands and, thus, strongly modifies the nature of the metallic state, despite the relatively small structural changes of the double layer.

Tight-binding extended Hückel calculations for ZrCl have already been reported by Corbett et al.[29] which showed that the results are in qualitative agreement with photoelectron spectroscopy data. Here we point out that the nature of the d-block bands can be qualitatively understood as arising from the interaction of the energy levels of an ML_3 fragment. As schematically shown in **3**, the ML_3 fragment possesses three

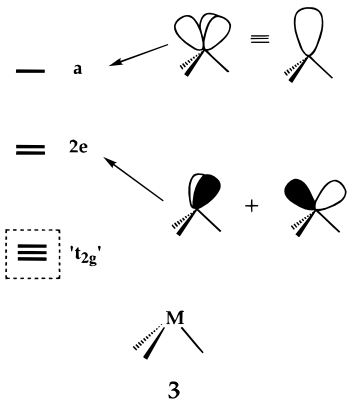

3

low-lying basically nonbonding orbitals, which are the remnants of the t_{2g} levels of an octahedron, and three higher lying orbitals (a + 2e) whose lobes are oriented toward the three vertexes of a hypothetical octahedron.[30] The three low-lying levels (which we will call "t_{2g}" in the following) mix and lead to three levels interacting with those of the second nearest neighbor Zr atoms (i.e., those at 3.42 Å), leading to six moderately dispersive bands. Within the ZrCl double layers, the a + 2e orbitals point directly toward the equivalent orbitals of the three nearest neighbor Zr atoms (i.e., those at 3.09 Å), leading to very strong interactions and thus to three bonding and three antibonding combinations. The three bonding ones lead to three low-lying bands that lie in the same region as the bottom part of the bands based on the t_{2g} orbitals. As a result there is a strong mixing between the two types of bands so that when six electrons fill the bottom of the d-block bands, Zr−Zr bonding among both first and second nearest neighbor Zr atoms results. Other descriptions, like those based on the condensation of cluster orbitals, may be more appropriate to describe the metal−metal bonding in ZrCl; however, in the context of the present discussion this one is probably more appropriate.

In β-ZrNCl the three Cl and three N atoms at 2.12 Å provide a local octahedral coordination (in fact it is better described as a trigonal antiprismatic coordination) for the Zr atoms, so that the three (a + 2e) levels will be kept high in energy (two of

(29) Ziebarth; R. P.; Hwu, S.-J.; Corbett, J. D. *J. Am. Chem. Soc.* **1986**, *108*, 2594.
(30) Albright, T. A.; Burdett, J. K.; Whangbo, M.-H. *Orbital Interactions in Chemistry*; John Wiley: New York, 1985; Chapter 20.

them will be the pseudo-e_g* Zr−N antibonding), and three levels, i.e., the three t_{2g} orbitals, will remain low in energy. One of these three, i.e., z^2, will be strongly raised because of the presence of the fourth N atom coordinated to Zr at 2.24 Å, i.e., the capping N, so that only two of the t_{2g} orbitals are left for metal−metal interactions. These four orbitals (two from each Zr atom) lead to four low-lying bands, two of which are the bottom of the d-block and are those which will be partially filled upon donor intercalation. These two bands exhibit dispersion (∼1.2 eV) because of both Zr−N and Zr−Zr orbital mixing. The bottom part of these bands is slightly Zr−Zr bonding and Zr−N antibonding as can be judged from the comparison of the overlap populations for β-ZrNCl reported above and those calculated for $Li_{0.4}$ZrNCl using a rigid band scheme: 0.019 for Zr−Zr (3.35 Å), 0.317 for Zr−N (2.12 Å), and 0.253 for Zr−N (2.24 Å). Thus, the partially filled bands of β-ZrNCl and ZrCl certainly have some common feature, i.e., they originate from the t_{2g} Zr orbitals, but the differences are much more significant, i.e., the destabilization of the z^2 orbital as well as the nonparticipation of the a + 2e orbitals which are largely responsible for the extended metal−metal bonding in the case of ZrCl.

The previous analysis makes clear an important point: the essential role played by the N atom at 2.24 Å in raising the z^2 orbital to higher energies. If it were not for this capping atom, the z^2 orbital would have been the lowest of the t_{2g} set leading to the partially filled (and quite narrow) band upon donor intercalation. In the crystal structure reported by Juza et al.[4] one of the Zr−N sublayers of the Zr−N−N−Zr double layer is shifted in such a way that the local environment of the Zr atoms does not contain the capping N atom. Thus, calculations based on the structure of Juza et al.[4] (see Figure 10c) would lead to incorrect results as far as the bottom of the d-block bands is concerned. Comparison of parts c and b of Figure 10 makes clear the presence of a narrow peak in the DOS of β-ZrNCl calculated according to the structure of Juza et al.[4] which is shifted around 3 eV when the redetermined structure is used. This explains the puzzling result reported by Woodward and Vogt[31] who carried out a theoretical study of β-ZrNCl before the redetermination of the crystal structure. As noted by these authors, it was quite puzzling that metallic conductivity (and even superconductivity) was realized upon electron transfer to quite narrow bands. Thus, in looking for correlations between T_c and the filling of the d-block bands or between T_c and structural details, it is absolutely necessary to use the newly determined crystal structure.

Before looking for possible relationships between T_c and the doping level, we comment on the Fermi surface and the adequacy of a rigid band scheme in studying the donor intercalated β-ZrNCl phases. The calculated Fermi surfaces for Li_xZrNCl as a function of x according to a rigid band scheme are shown in Figure 11a−d. These Fermi surfaces are closed and could be described as made up of "rounded triangles", although this shape is only barely recognizable for values of x around 0.2. At least for low doping levels, i.e., $x = 0.1-0.6$, there are not well-nested portions on these Fermi surfaces so that no Fermi surface driven electronic instabilities of the charge or spin density wave type are expected. This is in agreement with the normal metallic behavior exhibited by all alkali-metal-intercalated phases before entering the superconducting state. Just after $x = 0.6$ new features appear at the center of the Brillouin zone (see Figure 11d). It is interesting to note that Yamanaka et al.[2b] have reported that T_c (15 K) in A_xZrNCl (A = Li, Na, K) remains almost constant with increasing x from 0.1 to 0.5, while it drops to 10 K with a further increase in x. It is tempting to suggest that the two observations, i.e., changes in the Fermi surface and T_c for x around 0.5−0.6, may be correlated. However, we believe that some structural change occurring for high alkali metal contents may be a more likely origin for this drop in T_c.

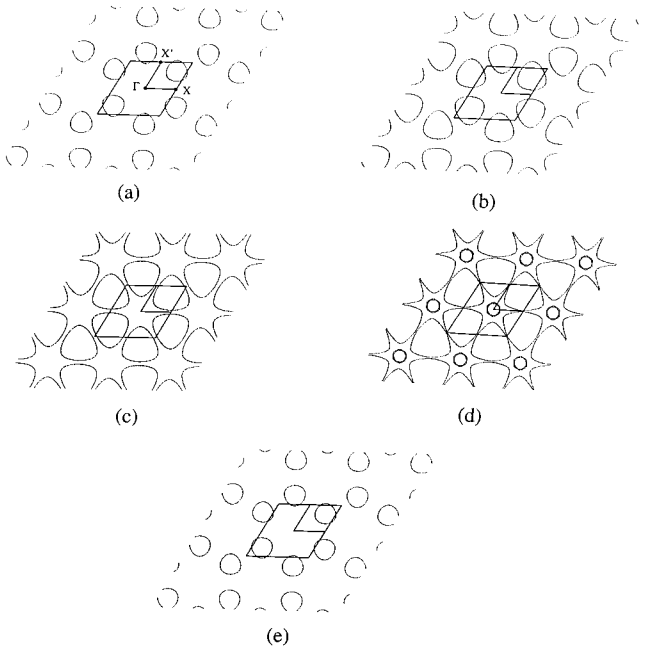

Figure 11. Calculated Fermi surface for Li_xZrNCl as a function of x using a rigid band scheme and the redetermined structure of β-ZrNCl: (a) $x = 0.2$, (b) $x = 0.4$, (c) $x = 0.6$, and (d) $x = 0.8$. (e) Calculated Fermi surface for $x = 0.2$ using the 4 K crystal structure of $Li_{0.16}$-ZrNCl.[6] $\Gamma = (0, 0)$, $X = (a^*/2, 0)$, and $X' = (0, a^*/2)$.

We have also repeated these calculations using the recent neutron diffraction structure of the lithiated phase $Li_{0.16}$ZrNCl determined at 4 K.[6] Although there are some important changes in the bond lengths and angles affecting the coordination environment of Zr induced by the presence of the lithium atoms in this structure, we find practically no difference between the Fermi surfaces calculated as a function of x using the $Li_{0.16}$-ZrNCl and β-ZrNCl structures (compare for instance the calculated Fermi surfaces for $x = 0.2$ in parts a and e of Figure 11). The only difference we observe is that the new features at the center of the Brillouin zone appear at slightly lower doping levels when the $Li_{0.16}$ZrNCl structure is used. Thus, we believe that, at least for not very high doping levels where, as commented, it is not clear if some structural change occurs, a rigid band scheme seems to be appropriate for studies of these phases. When the writing of this work was almost completed, Felser and Seshadri reported an LMTO study of the Fermi surfaces of these systems.[32] These Fermi surfaces are essentially similar to those reported here despite being based on different computational methods and crystal structures (i.e., they used the crystal structure of the isoelectronic $NaZr_2N_2ClS$ phase). The similarity of results makes us confident that the Fermi surfaces of Figure 11 are indeed the correct Fermi surfaces for these phases. Felser and Seshadri have also suggested that a van Hove type scenario could be appropriate to explain the superconductivity exhibited by these phases. We are rather skeptical about this proposal because it leads these authors to suggest that the maximum T_c in β-ZrNCl should be reached for x values around 0.55. However, as we mentioned above, a

(31) Woodward; P. M.; Vogt, T. *J. Solid State Chem.* **1998**, *138*, 207.

(32) Felser, C.; Seshadri, R. *J. Mater. Chem.* **1999**, *9*, 459.

T_c of 15 K is already found for values of x as low as 0.17 and is kept constant until around 0.5 (but see our comments below).[2b]

We also studied how changes in the nature of the halogen and the transition metal can affect the results by performing calculations for β-ZrNBr and β-HfNCl. The results are very similar to those for β-ZrNCl and thus are not reported here. Only slight differences in the band dispersion and energy gap were found.[3] More important for the present discussion is the fact that the calculated density of states at the Fermi level, $N(e_f)$, for a given value of x is quite similar for the three phases (at least for low doping levels, i.e., $x = 0.2-0.6$). Thus, assuming that the BCS scenario applies for these compounds, the considerably higher T_c reported for $Li_{0.48}HfNCl$ (23 K) with respect to $A_{\sim 0.48}ZrNCl$ (A = Li, Na, K) in the samples prepared by Yamanaka et al.[1,2] should be due to the existence of softer phonon modes in the former phase. We also note that whereas we found a continuous increase of $N(e_f)$ when x changes from 0.1 to 0.5, T_c remains constant according to the above-mentioned results of Yamanaka et al.[1,2] These authors also found a minimum change in T_c between 25.5 and 24 K for a wide range of lithium contents in Li_xHfNCl. All these results suggest that $N(e_f)$ does not play an important role in determining T_c. In contrast, we find T_c values of 18 and 24 K for samples of Li_x-HfNCl with lithium contents of 0.42 and 0.67, respectively. This fact does not necessarily imply that $N(e_f)$ is responsible for the apparent increase in T_c with x nor that the two sets of results are in contradiction. For instance, in our lithiated samples only lithium cations enter the van der Waals gap between the layers, occupying part of the holes and interacting strongly with the negatively charged halogen atoms. In some of the samples prepared by Yamanaka et al. solvent molecules are co-intercalated so that, according to the model proposed by these authors,[1] most of the lithium cations do not interact directly with the halogen atoms but with the solvent. This means that, for a given value of x, the phonon spectra of the layers are probably more strongly affected in our samples than in those prepared with solvent co-intercalation. If a phonon-mediated scenario is applicable, somewhat different x vs T_c dependencies could then be expected. Conversely, if the previous reasoning is correct, the fact that $Li_{0.16}ZrNCl$ and $Li_{0.16}(DMF)_yZrNCl$ or $Li_{0.17}ZrNCl$ and $Li_{0.17}ZrNBr$ exhibit practically the same T_c[2b,3] could be suggestive of some non-phonon-based mechanism. Whether these ideas play some role in this discussion is something that is not clear at this moment. We believe that this, as well as some other possible problems, like those related with the homogeneity of some samples or with their possible hydrogen content, must be clarified before correlations between x and T_c can be meaningfully discussed and give us a hint about the possible mechanism leading to the superconductivity in these phases.

Finally, since Yamanaka et al.[1] have commented on the structural relationship between the β-MNX phases and the $Ln_2C_2X_2$ family of compounds, for which superconductivity has also been reported,[33] we have also studied some compounds of this family. The calculated DOS for $Y_2C_2Br_2$ is reported in Figure 10d. The Fermi level lies around the middle of the contribution between -7.5 and -10 eV, which is mainly C_2 π^* in character with some admixture of the Y d orbitals. Thus, whereas for reasonable values of x in Li_xMNX the states near the Fermi level have mostly M character, those in $Y_2C_2Br_2$ originate predominantly from the C_2^{4-} group.[34] This is something that could have been derived just on the basis of electron counting arguments. The topology of their Fermi surfaces is also very different. Consequently, despite the structural analogies and the reported superconductivity in both systems, there is seemingly no relationship between their electronic structures.

Acknowledgment. This study was supported by the Spanish CICYT (Grant MAT96-1037-C02-02), DGES (Grants PB95-0848-C02-01 and PB96-5809), and the Comissionat per Universitats i Recerca de la Generalitat de Catalunya (CIRIT; Grants 1997-SGR24, 1997-SGR72, and 1996-SGR51). M.R.P. is grateful to the Generalitat de Catalunya for a RED contract. M.V. is grateful to the Ministerio de Educación y Cultura for a sabbatical leave fellowship. The authors also are grateful to Dr. Nieves Casañ-Pastor for the SQUID measurements.

IC9903127

(33) Simon, A.; Mattausch, H.; Eger, R.; Kremer, R. K. *Angew. Chem., Int. Ed. Engl.* **1991**, *30*, 1188.

(34) See also: (a) Miller, G. J.; Burdett, J. K.; Schwarz, C.; Simon, A. *Inorg. Chem.* **1986**, *25*, 4437. (b) Simon, A.; Yoshiasa, A.; Bäcker, M. R.; Henn, W.; Felser, C.; Kremer, R. K.; Mattausch, H. *Z. Anorg. Allg. Chem.* **1996**, *622*, 123.